RADIATION RESEARCH 147, 329–334 (1997)
0033-7587/97 $5.00

Measurement of Tumor Oxygenation: A Comparison between Polarographic Needle Electrodes and a Time-Resolved Luminescence-Based Optical Sensor

D. R. Collingridge, W. K. Young, B. Vojnovic, P. Wardman, E. M. Lynch, S. A. Hill and D. J. Chaplin

The Gray Laboratory Cancer Research Trust, P. O. Box 100, Mount Vernon Hospital, Northwood, Middlesex HA6 2JR, United Kingdom

Collingridge, D. R., Young, W. K., Vojnovic, B., Wardman, P., Lynch, E. M., Hill, S. A. and Chaplin, D. J. Measurement of Tumor Oxygenation: A Comparison between Polarographic Needle Electrodes and a Time-Resolved Luminescence-Based Optical Sensor. *Radiat. Res.* 147, 329–334 (1997).

A novel oxygen sensor which does not rely on electrochemical reduction has been used to measure the oxygenation of the murine sarcoma F in a comparative study with an existing polarographic electrode that is available commercially. The prototype luminescence sensor yielded an oxygen distribution comparable with readings made using a pO_2 histograph. The percentage of regions detected that had a pO_2 less than 5 mm Hg was 79 and 75 using the Eppendorf pO_2 histograph and the luminescence fiber optic sensor, respectively. These values were compatible with a measured radiobiologically hypoxic fraction of 67% in this tumor. The polarographic method detected more regions with a pO_2 of 2.5 mm Hg or less (69%) compared with the optical sensor (50%) ($P < 0.05$). This could reflect differences in the oxygen use of the sensing devices. This initial assessment indicates the potential of a fiber-optic-based oxygen-monitoring system. Such a system should have several advantages including monitoring temporal oxygen changes in a given microregion and use with NMR procedures.

INTRODUCTION

Microregional oxygen deficiency in human tumors is regarded as a major contributing factor in local radiation response (*1*). In particular, the proportion of cells existing at oxygen tensions between 0–10 mm Hg will be of importance, since radiosensitivity varies from its minimum to near maximum value over this range. Indeed, nearly three times more radiation dose is needed to kill hypoxic cells relative to normally aerobic cells (*2*). The measurement of tissue oxygenation is therefore of great clinical interest both as a predictive assay and as a means of understanding tumor pO_2, which may aid future treatment development for both radiotherapy and chemotherapy.

At present, the most commonly used commercial system for the measurement of tissue oxygenation *in vivo* is an electrode designed for rapid assessment of oxygen distribution throughout a tissue: the Eppendorf pO_2 histograph (*3*). This instrument relies on polarography. Clear advantages exist using this mode of measurement, for example a linear relationship between current and pO_2, and by optimizing the polarization voltage along with the addition of a Teflon membrane at the probe tip, contamination *in vivo* from molecules other than oxygen is reduced significantly. However, technically there are several potential limitations which can be minimized but not eliminated. These include the consumption of tissue oxygen by electrochemical reduction, which can introduce underestimation to the oxygen value. It should be noted that the Eppendorf histograph is designed to minimize this by incorporating a recessed tip electrode, a feature examined by Whalen *et al.* (*4*), and by moving the electrode progressively through the tissue. Nevertheless, oxygen depletion will still occur, albeit lower than that resulting from blunt-ended nonmovable electrodes of, for example, the original Clark design (*5*). A second technical problem involves the difficulties of accurately detecting the very small currents associated with low oxygen concentrations over and above the general background noise. This problem becomes more important as electrode geometry is miniaturized.

Theoretically, these limitations can be overcome using fiber-optic sensors which use dyes whose luminescence is quenched by oxygen. Essentially, these sensors rely on the measurement of the oxygen-quenched lifetime of a luminescent molecule immobilized at the tip of an optical fiber. The optical fiber is used to guide the excitation and emission light transients to the measurement system. However, as with the development of polarographic electrodes for routine use in living tissue, several technical challenges had to be overcome. These included the identification of a suitable luminophor, attachment of this to a fiber optic and the development of real-time signal analysis methods. Recent work at the Gray Laboratory has resulted in the development of a prototype device which uses the fluorophor, tris(4,7-diphenyl-1,10-phenanthroline) ruthenium chloride. Technical details and some preliminary measurements with the device have recently been reported (*6*, *7*).

The fiber-optic sensor operates most effectively in the 0–15 mm Hg pO_2 range with fast response and settling times (<2 s). The object of the current study was to evaluate the applicability of the device for measuring tumor oxygen tension and to compare the measurements to those obtained using the Eppendorf pO_2 histograph as well as to radiobiological measurements of hypoxia.

MATERIALS AND METHODS

Tumor Model

The tumor used in this investigation was the sarcoma F (SaF) murine tumor transplanted subcutaneously into the rear dorsum of female CBA/Gy f TO mice. These tumors were serially maintained by injecting 0.05 ml of a crude cell suspension and selected for treatment when they had reached 5–6 mm in diameter.

Measurement of Radiobiological Hypoxia

Tumor irradiation. All irradiations were performed using a 250 kV Pantak X-ray machine set at 240 kV and 15 mA. The mean dose rate for these series of experiments was 3.6 Gy/min. Tumors were irradiated in a similar fashion to the method originally developed by Sheldon and Hill (*8*). The mice were unanesthetized and exposed to either breathing air or hypoxia during irradiation. Hypoxia was induced by sacrificing the tumor-bearing mouse by cervical dislocation 10 min before the start of irradiation.

Clonogenic survival. Full details of this procedure have been published (*9*). Briefly, after irradiation the tumors were immediately excised, weighed, chopped and enzymatically digested (each dose point consisted of data from the pool of two tumors). After cell recovery and counting, known numbers of cells were dispensed into petri dishes and incubated at 37°C in a humidified incubator gassed with 2% O_2/5% CO_2/93% N_2 for 7–10 days. The colonies were fixed, stained with methylene blue and counted.

Calculation of hypoxic fraction. Colony-forming efficiency (CFE) was calculated by counting the number of colonies on the petri dish and dividing this by the number of cells originally seeded. Three dilutions were made of each sample and each dilution was duplicated; thus the average of six samples gave the average CFE for each group and a standard error on the mean was calculated. The surviving fraction (SF) was determined by calculating the number of clonogens per 100 mg of treated tumor and dividing this by the average number of clonogens per 100 mg of control tumor. The SFs of the aerobic and hypoxic treatments were plotted on a semi-log scale (radiation dose as a function of SF) with the best linear fit for the curve for hypoxic cells calculated. This fit was superimposed on the data for cells under aerobic conditions and the hypoxic fraction obtained from the vertical displacement of the curve for aerobic cells from the curve for hypoxic cells (*10*). To estimate the uncertainty on the hypoxic fraction, the ratios of the four paired dose points were averaged and the standard deviation of the mean was calculated.

pO_2 Measurements: Eppendorf Histograph

Principle of measurement. Full details are described elsewhere (*11*), but a brief description is given here. Oxygen partial pressure (tension) is measured by a 17-μm gold polarographic microelectrode contained in the recess of a 300-μm beveled steel needle probe which is covered by a Teflon membrane. It is polarized to –700 mV with respect to a Ag/AgCl anode which is attached to the skin or underlying musculature near the site where the probe is inserted. Oxygen electrodes work on the principle of electrochemical reduction of oxygen at the cathode (probe surface). The process of reduction results in the production of OH^- ions and requires a source of electrons supplied by the anode (*12*). The resulting current is proportional to the oxygen partial pressure at the electrode tip.

Measurement procedure. Unanesthetized tumor-bearing animals were restrained in Perspex jigs. Using a pO_2 histograph (Eppendorf KIMOC 6650, Hamburg, Germany) with a net step length of 0.6 mm, 40–70 measurements were made from 6 tracks through each tumor. The reference Ag/AgCl electrode (Medicotest UK Ltd., St. Ives, Cambridgeshire, UK) was attached to a shaved region on the back of each mouse to ensure a good electrical contact.

pO_2 Measurements: Fiber-Optic Sensor

Principle of measurement. Full details have been reported recently (*6*), but a brief summary is given here. Oxygen tension is measured by the change in lifetime of the luminescent (excited) state of a ruthenium luminophor incorporated in a silicone rubber polymer attached to the tip of an optical fiber with an external diameter of 230 μm. The luminophor is excited by 450 nm excitation light from a N_2-pumped dye laser and the fluorescence emission at 600 nm is detected using a photomultiplier tube. The lifetime of the luminescent signal is inversely proportional to oxygen tension. Oxygen tensions are obtained by comparing the observed lifetime (τ) to that obtained in the absence of oxygen (τ_0), using a modified Stern-Volmer-type model (*13*).

Calibration. The luminescence sensor was calibrated against the following combination of gases, N_2, 0.5% O_2, 2% O_2, 5% O_2 and 21% O_2, by placing the sensor into a series of deionized water solutions each bubbling with the appropriate oxygen concentration. Calibration measurements were made in a thermostatted bath set to 30°C to approximate the average tumor temperature. These lifetimes were used to obtain the coefficients for the model using a nonlinear least-squares method. The calibration would normally last for approximately 20 h of use before recalibration was needed. Before each measurement session, the lifetime at 0% O_2, τ_0, was measured and used in the model to estimate the oxygen tension.

Measurement procedure. Unanesthetized tumor-bearing animals were restrained in Perspex jigs. The fiber-optic sensor was inserted into the tumor through a small skin incision made with a 25-gauge needle. Each control animal was assessed at 12 different insertion sites. Measurements were performed for a minimum of 6 min at each site, which was sufficient to allow the sensor to equilibrate to the oxygen tension prior to obtaining a stable reading for the site. Data collection was made at a frequency of 15 readings per minute.

Data Analysis

Polarographic data. From the pO_2 values obtained for each tumor, the median and the percentage less than 2.5 mm Hg, less than 5 mm Hg and less than 10 mm Hg were calculated and averaged for the 35 animals involved. The oxygen distribution, expressed as a histogram, was calculated from the pooled data for all the animals.

Luminescence sensor data. An average pO_2 value for each 6-min trace was obtained, after allowing for sensor equilibration and stabilization, at each insertion site. This yielded 12 pO_2 values per tumor which were then analyzed in the same manner outlined for the polarographic data.

Statistical analyses. After the preliminary data analysis outlined above, each tumor had four oxygen values associated with it: median, percentage less than 2.5 mm Hg, percentage less than 5 mm Hg and percentage less than 10 mm Hg. By pooling these values for each of the oxygen parameters, a comparison between the polarographic and luminescence sensor data was performed using Student's *t* test for two independent populations with a significance of 95% ($P = 0.05$).

Necrotic Fractions

Tumors were excised, fixed in formalin, processed and embedded in paraffin. Sections 4 μm thick were cut at three levels throughout each tumor and stained with hematoxylin and eosin for histological examination. Using an eyepiece graticule and 20× magnification on a light microscope, the percentage of necrotic cells per section was calculated and averaged for a group of six tumors.

RESULTS

Figure 1 shows the radiation response data for tumors irradiated in air-breathing mice and for tumors rendered

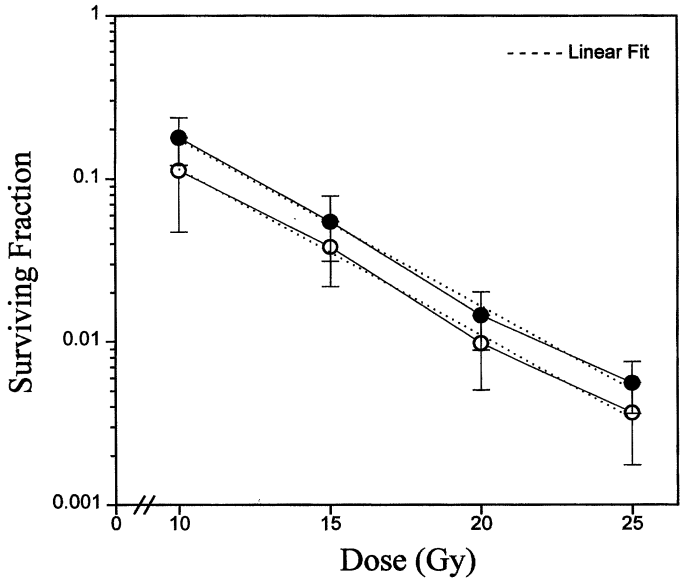

FIG. 1. Survival curves for SaF tumor cells irradiated *in vivo*. (●) Survival in tumors made 100% hypoxic during the radiation procedures (n = 8). (○) Survival in tumors unperturbed during the radiation treatment (n = 12). Hypoxic fraction, calculated from the displacement of the two lines as described in the Materials and Methods, equaled 66.6% (± 2.79). n = number of experiments. The data points are the mean ± 1 SEM.

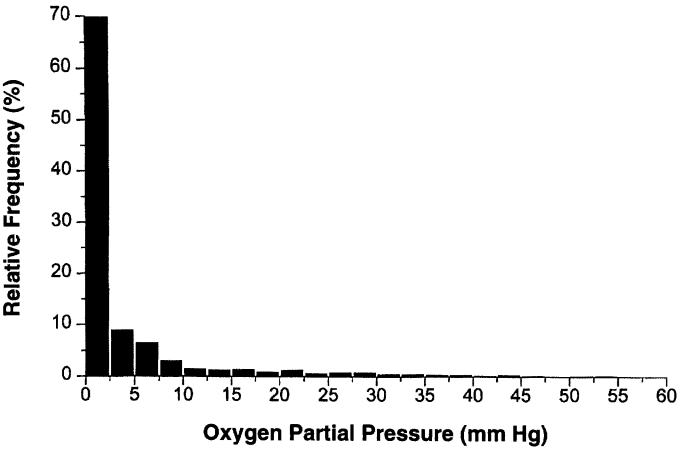

FIG. 3. pO_2 histogram representing the oxygenation of the sarcoma F murine tumor as determined polarographically. N = 35; n = 1981. (N = number of animals; n = number of measurements.)

100% hypoxic. It can be seen that the SaF tumor has a radiobiologically hypoxic fraction, assessed from the displacement of the two survival responses, of 67%. In clinical radiation oncology such measures of radiobiological hypoxia are impossible, and assessment has to be made using oxygen sensors. In the present study, we have assessed the oxygen tension in SaF tumors using two different oxygen sensors, namely the commercially available Eppendorf pO_2 histograph and an in-house fiber-optic luminescence sensor. The calibration curve for the latter is shown in Fig. 2. The curve illustrates a nonlinear response and is thus quite different from the well-established linear relationship between current and pO_2 obtained with polarographic measurements. This nonlinearity highlights an interesting feature of the fiber-optic device. The error in the lifetime (τ) reading will attribute varying degrees of error to the oxygen reading. At lower oxygen values of less than about 5%, the errors will be smaller than those attributed to readings of 21% oxygen: hence an increased accuracy at lower oxygen tensions. However, this does mean decreased accuracy at higher oxygen levels. (The linear response of a polarographic electrode ensures the same degree of uncertainty at any oxygen measurement.)

The histograms of pO_2 values obtained from SaF tumors using the Eppendorf pO_2 histograph and using the fiber-optic luminescence sensors are shown in Figs. 3 and 4, respectively. Both the histograph and luminescence

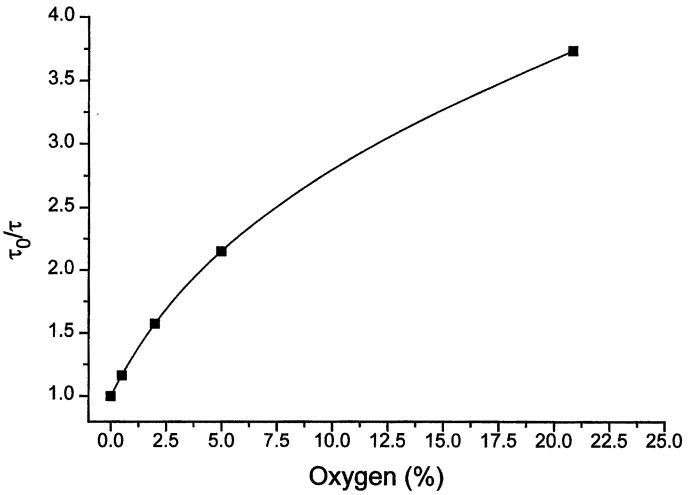

FIG. 2. Calibration curve for the fiber-optic oxygen sensor.

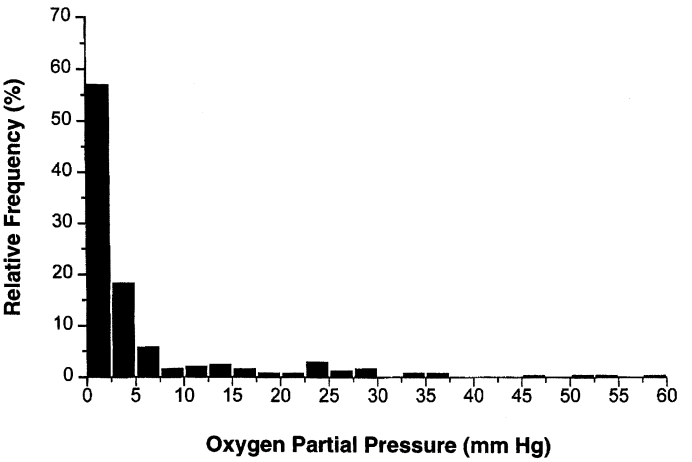

FIG. 4. The oxygen distribution of the sarcoma F as determined with the fiber-optic oxygen sensor. N = 20; n = 240. (N = number of animals; n = number of measurements.)

TABLE I
Measurement of Oxygenation of SaF Tumors Using Polarography and Fiber-Optic Technology

	Eppendorf pO_2 electrode ($N = 35, n = 1891$)		Luminescence sensor ($N = 20, n = 240$)	
	Value	SEM	Value	SEM
Median[a] (mm Hg)	1.4	0.3	2.8	0.5
Percentage <2.5 mm Hg[a]	68.8	4.6	49.6	7.6
Percentage <5.0 mm Hg	78.7	3.1	75.4	4.1
Percentage <10.0 mm Hg	88.7	1.6	82.9	3.2

Note. N = number of animals; n = number of measurements.
[a]Luminescence sensor and Eppendorf electrode measurements are significantly different ($P < 0.05$).

sensor identify a range of oxygen tensions from 0 to 60 mm Hg. However, the majority of values are in the range of 0 to 5 mm Hg, consistent with the existence of radiobiological hypoxia.

To assess whether the high proportion of values less than 2.5 mm Hg measured by both of these techniques could be attributed to sampling large regions of necrosis, a histological study was performed. From this the necrotic fraction was found to be very low at 8.3% (SEM ± 0.5) and thus would not be expected to have a major influence on the overall oxygen distribution.

A direct comparison of values obtained with the Eppendorf histograph and the fiber-optic sensor are shown in Table I. It can be seen that overall the values are broadly comparable. Indeed, the percentage of values less than 5 mm Hg (considered to be a measure of radiobiological hypoxia) is almost identical and furthermore is similar to the measured radiobiologically hypoxic fraction in this tumor. However, the median value obtained with the fiber-optic sensor is higher than that obtained with the Eppendorf histograph.

DISCUSSION

Hypoxia is known to be a key factor responsible for tumor resistance to radiation. *In vitro* studies have also indicated that it can induce resistance to chemotherapeutic drugs (*14–16*) and alter the cellular responses to cytokines (*17–19*). The advent of the Eppendorf pO_2 histograph has enabled clinical measurements of tumor oxygenation to be made. These studies have shown that hypoxia ($pO_2 <$ 10 mm Hg) is a common feature of solid tumors in humans (*20*). Moreover, hypoxia has been shown to be a prognostic indicator for local control after radiotherapy in head and neck and cervical cancer (*21*, *22*). Likewise, recent studies indicate that hypoxia can predict for distant metastasis and survival in patients with soft tissue sarcomas (*23*). These studies have shown that routine measurements of tumor hypoxia could be an important clinical assessment. The only device currently available for clinical measurements of tumor oxygenation is the Eppendorf histograph, which uses polarographic techniques for oxygen detection. Recent technical developments have indicated the potential of fiber-optic-based oxygen sensors (*6*, *7*).

The present study has provided the first direct *in vivo* comparison between a recently developed fiber-optic oxygen sensor and the established "gold standard" polarographic oxygen electrode, the Eppendorf histograph. The machines use two totally different processes to measure tissue oxygen tension. The calibration curve for the fiber optic, shown in Fig. 2, illustrates that, while measurements of oxygen tension over the physiological range are possible, increased accuracy at low oxygen tensions (<5%) is a fortuitous consequence of the luminophor's calibration behavior.

The electrode and the fiber-optic sensor both have similar dimensions with external diameters of 200–300 μm. The insertion of these sensors would be expected to result in similar tissue perturbation. The volume of measurement has been estimated for the Eppendorf as a region of 50–100 cells around the probe tip (*3*). The sampling volume of the fiber-optic sensor is difficult to estimate accurately. Further work is ongoing to examine the effect of the outer polymer coating upon the accuracy of oxygen measurement; however, it is expected that its contribution will be small and as such probe measurement should be confined primarily to the sensor tip. Coupled with the expected lower oxygen consumption by this technique, the sampling volume should be less than that of the Eppendorf histograph.

Despite the differences in the method of oxygen detection and the different methods of probe insertion and movement, the instruments provided very similar oxygen tension profiles in the murine sarcoma F. Based on previous radiobiological data, radioresistance is associated with pO_2 values less than 10 mm Hg and often less than 5 mm Hg. It can be seen that, if compared with the 67% radiobiologically hypoxic fraction actually measured, both sensors recorded percentages of values <5 mm Hg almost identical with this (79% for Eppendorf histograph and 75% for the optical sensor). However, there are some slight but significant differences in the measurements made by the two sensors when other parameters are compared. For example, the median pO_2 obtained for the tumors using the fiber optic or the Eppendorf are signifi-

cantly different (2.8 compared to 1.4 mm Hg). This reflects the fact that significantly more readings in the 0–2.5 mm Hg range are detected using the Eppendorf polarographic electrode. While this may be due to sampling differences, oxygen use may be another contributing factor, particularly when comparing a process of measurement that can induce a small degree of depletion with one whose oxygen consumption is probably lower.

This initial study has demonstrated the feasibility of using fiber-optic sensors for detection of tissue oxygenation. Further work is now required in other systems to demonstrate their utility. It is clear that a fiber-optic-based system could offer several advantages over a polarographic method. These include the ability to adapt the system to a multichannel device enabling the detection of temporal changes in tumor oxygenation on a microregional scale, an application that is difficult because of the oxygen use associated with polarographic electrodes.

In summary, these results indicate that the same degree of accuracy regarding oxygen measurement can be obtained with luminescence-based optical oxygen sensors as with polarographic electrodes. The optical sensor used in the current study had an external diameter of 230 μm compared with the Eppendorf needle electrode (300 μm). However, it is possible to develop fiber-optic probes with smaller diameters, thus reducing the degree of tissue damage induced by probe insertion and movement. At present the fiber-optic sensor is not automated to advance through tissue in a manner comparable with the Eppendorf histograph. While this aspect is a major drawback since sampling differences may contribute to a less rigorous average of the overall tissue oxygenation, work is ongoing to allow the addition of a stepper device similar to the histograph. Furthermore, with the expansion into a multi-sensor arrangement, the instrument could provide an oxygen-sensing device with improved clinical potential. However, as with the Eppendorf, the measurement process remains invasive, even if smaller-diameter probes are used. Clearly, the ideal routine clinical procedure should be noninvasive. Much effort is ongoing into the development of such procedures, particularly using magnetic resonance (MR) imaging (*24*, *25*). If such efforts succeed, the development and calibration of these imaging procedures will, in turn, require MR-compatible sensors. Fiber-optic devices, such as the one described here, being nonmagnetic and nonconducting, are ideally compatible with MR technology.

ACKNOWLEDGMENTS

This work was supported by the Cancer Research Campaign (CRC). DRC is funded by a Mount Vernon and Watford Hospitals Trust Studentship award. EML is funded by a Scott of Yews Studentship. The authors would like to thank Mr. P. Russell and his staff for care of the animals in this study.

Received: September 12, 1996; accepted: November 11, 1996

REFERENCES

1. R. H. Thomlinson and L. H. Gray, The histological structure of some human lung cancers and the possible implications for radiotherapy. *Br. J. Cancer* **9**, 539–549 (1955).
2. L. H. Gray and O. C. A. Scott, Oxygen tension and radiosensitivity of tumours. In *Oxygen in the Animal Organism*, pp. 537–553. Pergamon Press, Oxford, 1964.
3. H. B. Stone, J. M. Brown, T. L. Phillips and R. M. Sutherland, Oxygen in human tumors: Correlations between methods of measurement and response to therapy. *Radiat. Res.* **136**, 422–434 (1993). [Meeting Report]
4. W. J. Whalen, J. Riley and P. A. Nair, Microelectrode for measuring intracellular pO_2. *J. Appl. Physiol.* **23**, 798–801 (1967).
5. L. C. Clark, Monitor and control of blood and tissue oxygen tensions. *Trans. Am. Soc. Int. Org.* **2**, 41–48 (1956).
6. W. K. Young, B. Vojnovic and P. Wardman, Measurement of oxygen tension in tumours by time-resolved fluorescence. *Br. J. Cancer* **74** (Suppl. XXVII), S256–S259 (1996).
7. W. K. Young, B. Vojnovic and P. Wardman, Fibre optic sensor for oxygen measurement in tumours. In *Medical and Fiber Optic Sensors and Delivery Systems* (N. I. Croitoru, M. Miyagi, A. V. Scheggi and H. J. M. C. Sterenborg, Eds.), pp. 56–63. SPIE–International Society for Optical Engineering, Washington, DC, 1996.
8. P. W. Sheldon and S. A. Hill, Hypoxic cell radiosensitisers and local control by x-ray of a transplanted tumour in mice. *Br. J. Cancer* **35**, 795–808 (1977).
9. C. S. Parkins, S. A. Hill, S. J. Lonergan, M. R. Horsman, J. A. Chadwick and D. J. Chaplin, Ischemia induced cell death in tumors: Importance of temperature and pH. *Int. J. Radiat. Oncol. Biol. Phys.* **29**, 499–503 (1994).
10. J. E. Moulder and S. Rockwell, Hypoxic fractions of solid tumours: Experimental techniques, methods of analysis, and a survey of existing data. *Int. J. Radiat. Oncol. Biol. Phys.* **10**, 695–712 (1984).
11. P. Vaupel, K. Schlenger, C. Knoop and M. Hockel, Oxygenation of human tumours: Evaluation of tissue oxygen distribution in breast cancers by computerized O_2 tension measurements. *Cancer Res.* **51**, 3316–3322 (1991).
12. I. A. Silver, Polarography and its biological applications. *Phys. Med. Biol.* **12**, 285–299 (1967).
13. W. Xu, J. M. Demas and B. A. DeGraff, Highly luminescent transition metal complexes as sensors. In *OE/LASE—Biomedical Fibre Optic Instrumentation* (J. A. Harrington, D. M. Harris, A. Katzir and F. P. Milanovich, Eds.), Vol. 2131, pp. 417–425. Society of Photo-optical Instrumentation Engineers, Los Angeles, 1994.
14. E. Smith, I. J. Stratford and G. E. Adams, Cytotoxicity of adriamycin on aerobic and hypoxic Chinese hamster V79 cells *in vitro*. *Br. J. Cancer* **2**, 568–573 (1980).
15. B. A. Teicher, J. S. Lazo and A. C. Sartorelli, Classification of antineoplastic agents by their selective toxicities toward oxygenated and hypoxic tumor cells. *Cancer Res.* **41**, 73–81 (1981).
16. K. Sakata, T. T. Kwok, B. J. Murphy, K. R. Laderoute, G. R. Gordon and R. M. Sutherland, Hypoxia-induced drug resistance: Comparison to P-glycoprotein-associated drug resistance. *Br. J. Cancer* **64**, 809–814 (1991).
17. L. E. Sampson and D. J. Chaplin, The influence of microenvironment on cytotoxicity of TNF-α *in vitro*. *Int. J. Radiat. Oncol. Biol. Phys.* **29**, 467–471 (1994).
18. D. Loeffler, P. Juneau and S. Masserant, Influence of tumour physico-chemical conditions on interleukin-2-stimulated lymphocyte proliferation. *Br. J. Cancer* **66**, 619–622 (1992).
19. T. Aune and S. Pogue, Inhibition of tumour cell growth by interferon-γ is mediated by two distinct mechanisms dependent upon oxygen tension: Induction of tryptophan degradation and depletion

of intracellular nicotinamide adenine dinucleotide. *J. Clin. Invest.* **84**, 863–875 (1989).

20. P. Vaupel, Oxygenation of human tumours. *Strahlenther. Onkol.* **166**, 377–386 (1990).

21. M. Hockel, C. Knoop, K. Schlenger, B. Vorndran, E. Baubmann, M. Mitze, P. G. Knapstein and P. Vaupel, Intertumoral pO_2 predicts survival in advanced cancer of the uterine cervix. *Radiother. Oncol.* **26**, 45–50 (1993).

22. M. Nordsmark, M. Overgaard and J. Overgaard, Pretreatment oxygenation predicts radiation response in advanced squamous cell carcinoma of the head and neck. *Radiother. Oncol.* **41**, 31–39 (1996).

23. D. M. Brizel, S. P. Scully, J. M. Harrelson, L. J. Layfield, J. M. Bean, L. R. Prosnitz and M. W. Dewhirst, Tumour oxygenation predicts for the likelihood of distant metastases in human soft tissue sarcoma. *Cancer Res.* **56**, 941–943 (1996).

24. J. E. Fishman, P. M. Joseph, M. J. Carvlin, M. Saaid-Elmandjra, B. Mukherji and H. S. Sloviter, *In vivo* measurements of vascular oxygen tension in tumours using MRI of a fluorinated blood substitute. *Invest. Radiol.* **24**, 65–71 (1989).

25. C. L. McCoy, D. J. O. McIntyre, S. P. Robinson, E. O. Aboagye and J. R. Griffiths, Magnetic resonance spectroscopy and imaging methods for measuring tumour and tissue oxygenation. *Br. J. Cancer* **74** (Suppl. XXVII), S226–S231 (1996).